

## Effects of 8-hydroxyquinoline-coated graphene oxide on cell death and apoptosis in MCF-7 and MCF-10 breast cell lines

Firoozeh Kheiltash<sup>1</sup>, Kazem Parivar<sup>1\*</sup>, Nasim Hayati Roodbari<sup>1</sup>, Behnam Sadeghi<sup>2</sup>, Alireza Badiei<sup>3</sup>

<sup>1</sup> Department of Biology, Science and Research Branch, Islamic Azad University, Tehran, Iran

<sup>2</sup> Cancer Immunotherapy and Regenerative Medicine, Breast Cancer Research Center, Motamed Cancer Institute, ACECR, Tehran, Iran

<sup>3</sup> School of Chemistry, College of Science, University of Tehran, Tehran, Iran

### ARTICLE INFO

**Article type:**  
Original article

**Article history:**  
Received: Jun 21, 2019  
Accepted: Jan 28, 2020

**Keywords:**  
8-Hydroxyquinoline  
Apoptosis  
Breast cancer  
Cytotoxicity  
Graphene oxide

### ABSTRACT

**Objective(s):** Breast cancer is a devastating disease related to women. The anticancer properties of 8-hydroxyquinoline (8HQ) and the increasing use of graphene oxide (GO), as a drug delivery system with anti-cancerous properties, led us to investigate the toxicity and apoptosis-induction capability of 8HQ-coated GO on breast cancer cells compared with normal breast cells.

**Materials and Methods:** Breast cancer (MCF-7) and normal breast (MCF-10) cell lines were treated with several doses of 8-HQ-coated GO for 12, 24, and 48 hr. The toxicity of the nanocomposite was measured using MTT assay and the effect of the nanocomposite on cell apoptosis was determined by examining the expression of *P53*, *P21*, *Bax*, and *BCL2* genes, as well as Annexin-V /PI apoptosis assay.

**Results:** There were significantly increased cell deaths in nanocomposite-treated MCF-7 breast cancer cells, compared with treated normal breast cells. Significantly increased expression of *P53*, *P21*, and *Bax* genes and reduced expression of *BCL2* gene were found in the treated breast cancer cell line compared with the normal cell line. Annexin-V/PI assay also illustrated significant induction of apoptosis in MCF-7 following nanocomposite treatment.

**Conclusion:** Overall, 8HQ-coated GO has toxicity for breast cancer cell lines and one of the mechanisms through which this nanocomposite can induce cell death is the induction of apoptosis. With complementary *in vitro* and *in vivo* studies, this nanocomposite can be suggested as a nano-drug with anti-cancer properties.

### ► Please cite this article as:

Kheiltash F, Parivar K, Hayati Roodbari N, Sadeghi B, Badiei AR. Effects of 8-hydroxyquinoline-coated graphene oxide on cell death and apoptosis in MCF-7 and MCF-10 breast cell lines. *Iran J Basic Med Sci* 2020; 23:871-878. doi: 10.22038/ijbms.2020.41277.9751

### Introduction

Breast cancers in women are some of the major causes of death worldwide. Global cancer incidence is estimated at 18.1 million and about 9.6 million deaths in 2018 (1). Different therapies exist based on the type of cancer and its progression, including surgery, chemotherapy, radiotherapy, hormone therapy, and immunotherapy (2). Apoptosis is one of the main mechanisms to eradicate cancerous cells and inhibit this process by increasing anti-apoptotic proteins and decreasing pro-apoptotic proteins, resulting in the survival of cancer cells (3). That is why apoptosis has attracted a lot of attention in anti-cancer research. The *BCL2* protein family plays an important role in mitochondrial-dependent apoptosis. The members of this family are divided into two main groups of pro-apoptotic and anti-apoptotic proteins. The members of pro-apoptotic, especially *Bax*, play an important role in the onset of apoptosis (4). On the other hand, *P53* protein is an important protein in inducing apoptosis in damaged or cancerous cells. The activated *P53* binds to DNA and induces the expression of some genes, including *P21* (5). The *P21* protein by binding to the cell cycle complexes inhibits cell cycle and cell proliferation and acts as a stop signal in cell division. In contrast, anti-apoptotic members, such as *BCL2*, prevent

the onset of apoptosis by suppression of pro-apoptotic proteins, increasing cell survival, and promoting the cell cycle process (6, 7).

The specific feature of nanoparticles that increased their application in medical sciences as drug delivery systems is the high ratio of surface to volume. Carbon nanostructures have unique physicochemical properties that make them an important family in the field of nanomedicine (8). Graphene is a two-dimensional carbon allotrope consisting of hexagonal structures like a honeycomb with the thickness of an atom. This transparent nanoparticle has become one of the hottest topics in the fields of physics, chemistry, and nanotechnology. Graphene is the hardest and thinnest substance ever produced by human beings (9). Graphene oxide (GO) is obtained from complete oxidation and peeling of graphite, which includes a wide range of reactive oxygen groups containing epoxy, hydroxyl, carbonyl, and carboxyl groups. These reactive groups at the surface of GO make it soluble and increase the affinity to bond with other substances and drugs (10, 11).

Quinoline is an aromatic nitrogen compound that has various derivatives with a wide application range (12). One of these derivatives is 8-hydroxyquinoline

\*Corresponding author: Kazem Parivar. Department of Biology, Science and Research Branch, Islamic Azad University, Daneshgah Blvd, Simon Bolivar Blvd, Tehran, Iran. Email: Kazem.parivar@yahoo.com

(8-HQ), which has the ability to form complexes with bivalent metallic ions and has the potential to interfere with cancerous cellular pathways providing anti-cancer properties (13). 8-HQ and its derivatives have been used in medicine as anticancer, antioxidant, antimicrobial, anti-inflammatory, and anti-neurodegenerative agents. Its anticancer properties include prevention of cancer cell proliferation and tumor angiogenesis and induction of apoptosis in cancerous cells (13, 14).

The anticancer properties of 8-HQ and the increasing use of GO nanocomposites as drug carriers as well as its anti-cancerous properties (15), led us to use GO as the carrier of 8-HQ and investigate the anticancer properties of 8-HQ-coated GO by evaluating the toxicity and apoptosis-induction capability of this nanocomposite on breast cancer cells compared with normal breast cells.

## Materials and Methods

### Synthesis of nanocomposites

GO was prepared by oxidizing graphite powder according to the improved Hummers method (16). In summary, 0.5 g of graphite powder (Sigma Aldrich, USA) and 0.3 g of sodium nitrate (Sigma Aldrich, USA) were added to 16.5 ml cold sulfuric acid (Merck, Germany). The suspension was blended for a period of 20 min at a rate of about 150 RCF. After reaching the temperature to 0 °C in an ice bath, 1.5 g of potassium permanganate (Sigma Aldrich, USA) was added gradually over a period of 30 min to prevent sudden temperature rise. 30 ml of deionized water was slowly added to the suspension and 2 ml of hydrogen peroxide (Merck, Germany) was added dropwise. The suspension was washed several times with hydrochloric acid (Merck, Germany) and ethanol and centrifuged at 1800 RCF. The product was let to dry.

8-HQ used in this study was activated and bonded to mesoporous silica SBA-15, according to the protocol presented by Badieli *et al.* (17). To bind GO to silica-bound 8-HQ, 20 mg of GO was dissolved in 5 ml of dimethylformamide (Merck, Germany) and 50 mg of 4-dimethylaminopyridine (Merck, Germany) and 50 mg of N,N'-dicyclohexylcarbodiimide (Merck, Germany) were added and mixed at room temperature for 30 min. 30 mg of SBA-15-bounded 8-HQ was dissolved in 3 ml of dimethylformamide (Merck, Germany) in the presence of 1 ml of 10% hydrochloric acid (Merck, Germany). Then, the GO mixture was added and mixed overnight at room temperature. The solid phase was separated by centrifugation and washed twice with dimethylformamide and once with methanol (Merck, Germany). The resulting deposition was dissolved in 10 ml of deionized water and sonicated for 3 min using an ultrasonic system (Elma Ultrasonic, Germany). The detailed synthesis procedure, as well as the physicochemical properties of the nanocomposite such as its TEM and SEM view, were published previously (18).

### Treatment of breast cell lines with nanocomposite

$1 \times 10^4$  cells of each MCF-7 breast cancer cell line (ATCC, USA) and normal breast epithelial cell line (MCF-10A) (ATCC, USA) were cultured triplicate in 200  $\mu$ l of DMEM (Gibco, USA) containing 10% FBS (Gibco, USA)

and 1% penicillin-streptomycin (Gibco, USA) in two 96-wells plates (SPL, Korea) and nanocomposites were added at concentrations of 0.031, 0.062, 0.125, 0.25, and 0.5 mg/ml. There was no addition of the nanocomposite in the control wells. Plates were kept at a cell-culture incubator for 12, 24, or 48 hr.

### MTT and viability assay

Twenty microliters of MTT solution (Invitrogen, USA) with a concentration of 0.5 mg/ml was added to each well and plates were incubated for 4 hr in the dark. The supernatant was then discarded and 150  $\mu$ l DMSO (Merck, Germany) was added to the solution. The optical density of the produced dye at a wavelength of 570 nm was measured using an ELISA reader (BioTek, USA) and the percentage of live cells was calculated. The viability test was performed using trypan blue dye (Sigma, UK) for the cells treated with 0.5 mg/ml of the nanocomposite for 48 hr. The percentages of dead and live cells were measured by counting cells with Neobar Lam (HBG, Germany) and a light microscope (Zeiss, Germany).

### Study of apoptosis in nanocomposite-treated cell lines

#### Evaluation of BAX, BCL2, P53 and P21 gene expressions

The cell lines were treated with a concentration of 0.5 mg/ml of the nanocomposite for 48 hr. The cells were transferred to RNase-free microtubes and centrifuged for 5 min at 250 RCF and the supernatant was discarded. Total RNA was extracted using an RNA extraction kit (RNeasy mini kit Qiagen, Germany) according to the manufacturer's instructions. The quantity and quality of the extracted RNA were determined by measuring the absorbance of the RNA samples at 260, 230, and 280 nm using a PicoDrop (Spectrometer pico-drop, UK), and also 2  $\mu$ l of RNA was electrophoresed on agarose gel 1%. Synthesis of cDNA using a cDNA synthesis kit (RevertAid first-strand cDNA synthesis, Fermentas, Thermo Fisher Scientific, USA) was performed according to the kit instructions. Briefly, 9  $\mu$ l of extracted RNA plus 1  $\mu$ l of random hexamer primer, 4  $\mu$ l of reaction buffer, 1  $\mu$ l of RNase inhibitor, 2  $\mu$ l of dNTP (10 mM), and 1  $\mu$ l of reverse transcriptase enzyme were added together and supplemented with nuclease-free water to reach 20  $\mu$ l. Microtubes were placed in a thermal cycler (PeQlab, Germany) for 5 min at 25 °C, 60 min at 42 °C, and 5 min at 70 °C. The cDNA was dissolved in nuclease-free water and kept at -20 °C.

For qRT-PCR reaction, the  $\beta$ -actin gene was used as a reference gene and the primers used in this study are shown in Table 1 (19). 28 ng of the synthesized cDNA was added to a mixture containing 4  $\mu$ l Quantifast SYBR Green master mix (Qiagen, Europe) and 0.5  $\mu$ M of each of forward and reverse primers and the final volume was supplemented to reach 20  $\mu$ l. The samples were then placed in a rotor gene 6000 real-time rotary analyzer (Corbett life science, Australia) and after 10 min of initial denaturation at 95 °C, samples were amplified during 40 cycles each comprising 30 sec at 95 °C, 30 sec at 59 °C, and 45 sec at 72 °C. The Livak method was used to analyze gene expression (20).

### Apoptosis evaluation by Annexin-V/PI assay

The cell lines were treated with 0.5 mg/ml

Table 1. Primers used in the study of the apoptosis-related genes expression

Primer	Nucleotide sequence 5' → 3'	Ta	Product size (bp)	Ref. No
BAX (F)	5'-ACCAAG CTGAGCGA GTGTC-3'	60°C	293	18
BAX (R)	5'-ACAAAGATGGTCACGGTCTGCC-3'	60°C	293	18
BCL2 (F)	5'-ACCAAG CTGAGCGA GTGTC-3'	60°C	415	18
BCL2 (R)	5'-ACAAAGATGGTCACGGTCTGCC-3'	60°C	415	18
P53 (F)	5'-GTTCCGTCGGGCTTCTTG-3'	64°C	473	18
P53 (R)	5'-CTGGGCATCCTTGAGTTCC-3'	64°C	473	18
P21 (F)	5'-CTCAGAGGAGGCCCATG-3'	60°C	517	18
P21 (R)	5'-GGGCGGATTAGGGCTTC-3'	60°C	517	18
$\beta$ -actin (F)	5'-AACCGGAGAAGATGACCCAGATCATGTTT-3'	60°C	350	18
$\beta$ -actin (R)	5'-AGCAGCGTGGCCATCTCTGCTCGAAGTC-3'	60°C	350	18

F: Forward; R: Reverse; bp: Base pair

nanocomposite for 48 hr. The cells were washed twice with cold PBS and dissolved in 5 ml of binding buffer containing 5  $\mu$ l of each of annexin-V-FITC (BD, USA) and PI (BD, USA) with the concentration of 250  $\mu$ g/ml. After 15 min of incubation in the dark, samples were read using a flowcytometer (FACSCalibur, BD, USA).

### Statistical analyses

All tests were performed in triplicate. The Flowjo (Treestar) software was used to analyze and show the flow cytometric results. SPSS (version 19) and PRISM 7 software packages were used for statistical analysis and  $P$ -value<0.05 was considered significant. The data were described as mean with standard deviation. Analysis of variance (One-way ANOVA) was used to compare more than two quantitative variables.

## Results

### Evaluation of nanocomposite cytotoxicity by MTT and viability assays

MCF-7 and MCF-10 cell lines were treated with different concentrations of the nanocomposite in three periods of 12, 24, and 48 hr, and MTT assay was performed to study the toxicity of the nanocomposite. The percentages of live cells of each cell line at each concentration of drug treatment for 12, 24, and 48 hr are presented in Figure 1.

The results show that the percentages of viable cells in both normal and cancer cell lines treated with any concentration (0.031, 0.062, 0.125, 0.25, and 0.5 mg/ml) of the nanocomposite for any period (12, 24, and 48 hr) has significantly decreased compared with the related untreated control. The decreasing rate of cell viability was dose-dependent such that with increasing nanocomposite concentration, the mortality rate of cells also increased. Nevertheless, the results show higher cell death rate in the MCF-7 cell line, compared with the MCF-10 cell line, which is statistically significant at the concentration of 0.5 mg/ml of the nanocomposite. In 24 hr treatment, the mortality rates of the MCF-7 cell line at concentrations of 0.062, 0.25, and 0.5 mg/ml of the nanocomposite were significantly lower than those of MCF-10 cell line. Most differences in cell death are seen after 48 hr of treatment with different concentrations of nanocomposites such that there are significant lower mortality rates in MCF-7 cancer cell lines compared with normal MCF-10 cell lines at all concentrations of treatment with the nanocomposite, except for the concentration of 0.031 mg/ml. Figure 2 shows the trend of cell viability based on treatment

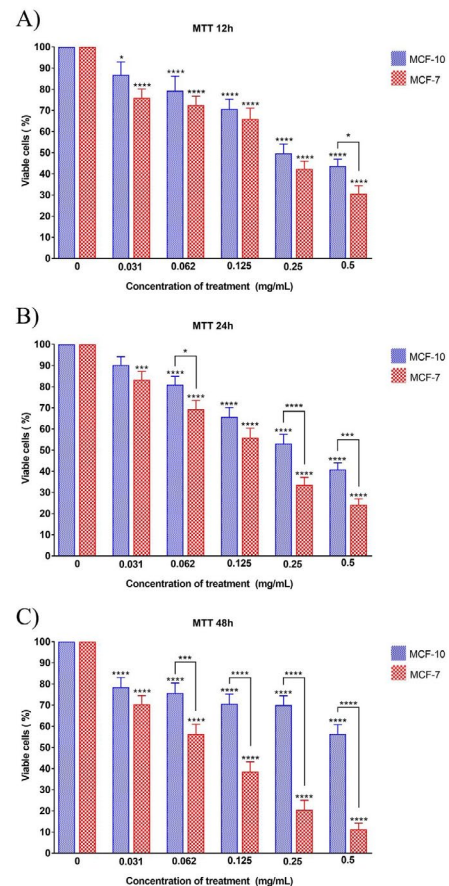


**Figure 1.** Bar chart of viable cell lines after exposure to five concentrations of nanocomposite for 12, 24, and 48 hr. The stars on each column indicate a significant difference compared with the related control (untreated cells) and the stars on the lines indicate a significant difference between the different treated cell lines.  $P$ -value<0.05:\*,  $P$ -value<0.01:\*\*,  $P$ -value<0.001:\*\*\*,  $P$ -value<0.0001:\*\*\*\*

time and concentration. As illustrated, increasing the time of treatment in almost all cases decreased cell viability. Moreover, in some treatment concentrations, 48 hr treatment significantly decreased cell viability, compared with 12 hr and 24 hr treatments. No significant difference was found between the viability percentages of 12 hr and 24 hr treated cells.

To show the maximum cytotoxic effect of the nanocomposite, all the remaining experiments were performed using 48 hr exposure of cells to 0.5 mg/ml nanocomposite. The results of calculating the

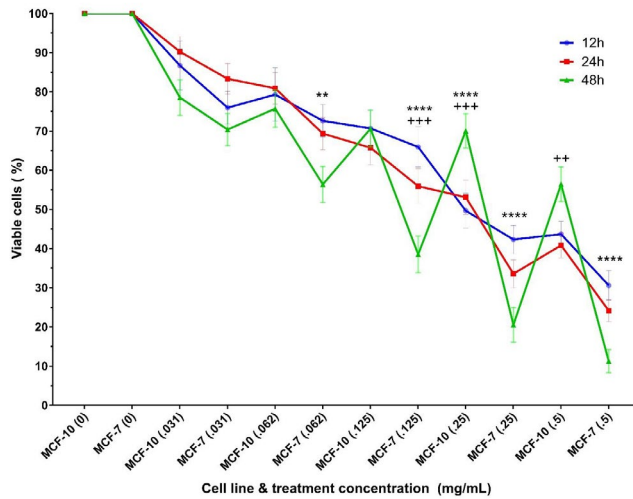


**Figure 2.** Trend of nanocomposite cytotoxicity on cell lines after exposure to five concentrations of nanocomposite for 12, 24, and 48 hr. The blue, red, and green lines are representative for 12, 24, and 48 hr treatments, respectively. Stars indicate significant differences in the viability of cells between 12 hr and 48 hr exposure to the nanocomposite. The plus signs indicate a significant difference in the viability of cells between 24 hr and 48 hr exposure to the nanocomposite. *P*-value<0.01:\*\*, *P*-value<0.001:\*\*\*, *P*-value<0.0001:\*\*\*\*

percentage of live cells after 48 hr exposure to 0.5 mg/ml of nanocomposite using trypan blue viability assay are shown in Figure 3. The results indicate that the percentages of viable cells in both cell lines decreased significantly compared with their untreated control samples. Also, there were significant differences in the percentages of cell death among breast normal and cancer cell lines. The MCF-7 cell line had significantly higher cell death (92%) compared with cell death in the normal MCF-10 cell line, which was about 45%.

**Evaluation of apoptosis in nanocomposite-treated cell lines**

*Measurement of Bax, BCL2, P53, and P21 gene expressions*

The optical absorption ratios of 260/280 and 260/230 nm were determined and samples with ratios between 1.8-2 were selected. Observation of the 18S and 28S bands, and the double strength of 28S to the 18S band, as well as the absence of smear on agarose gel, showed the purity and integrity of RNA. After confirming the quantity and quality of extracted RNA, cDNA was synthesized from RNA and expression of *P53*, *P21*, *BAX*, and *BCL2* genes was measured using the realtime-PCR method. The  $\beta$ -actin gene was used as the reference gene. Experiments were carried out in triplicate and the results were analyzed using the Livak formula. The expression level of the genes in MCF-10 cells was assumed as the reference and the expression of the genes in the MCF-7 cancer cell line was compared with those of MCF-10 and shown in Figure 4.

The results indicate that the expression of *P53*, *P21*, and *BAX* genes was significantly increased in MCF-7 cancer cell line compared with MCF-10. The expression level of *P53*, *P21*, and *BAX* genes in the MCF-7 cell line was approximately 4.4, 2.3, and 1.6 folds higher than those in the MCF-10 cell line, respectively. In contrast,

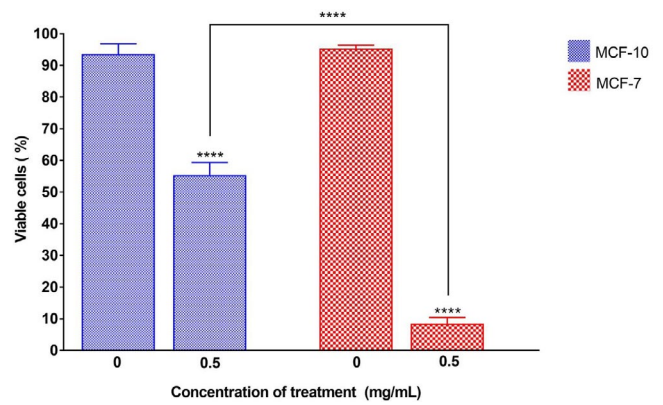


**Figure 3.** Percentage of viable cell lines after 48 hr of exposure to 5 mg/ml of the nanocomposite. The stars on each column show a significant difference compared with the related untreated control, and the interconnected lines indicate a significant difference between the different treated cell lines. *P*-value<0.0001:\*\*\*\*

the expression level of the *BCL2* gene in the MCF-7 cell line was significantly reduced to one-third of the *BCL2* expression level in the normal MCF-10 cell line.

*Apoptosis evaluation by Annexin-V/PI assay*

To determine whether the reduction of viable cell lines following treatment with the nanocomposite is apoptosis-mediated, the release of phosphatidylserine at the cell surface after 48 hr of treatment with 0.5 mg/ml of the nanocomposite was analyzed by Annexin-V-FITC/PI staining and flow cytometric analysis. The results are shown in Figure 5.

As shown in Figure 5, 99.28% of untreated MCF-10 cells were alive and only 0.56% of cells were necrotic. 0.09% and 0.08% of cells were in the early and late stages of apoptosis, respectively; cumulatively 0.17% of the cells were apoptotic.

After treatment of MCF-10 cells with 0.5 mg/ml of nanocomposite for 48 hr, 53.62% of the cells were alive

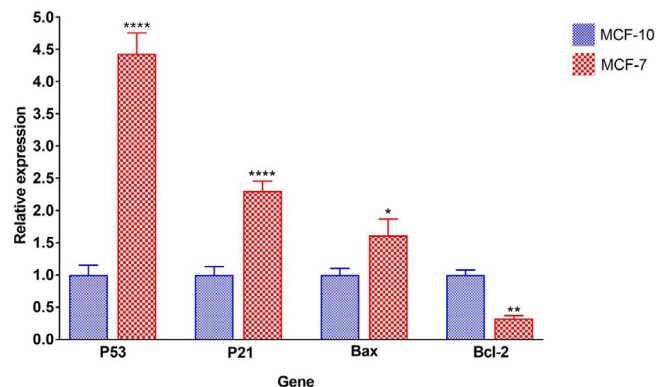


**Figure 4.** Relative expression of *P53*, *P21*, *Bax*, and *Bcl-2* genes in MCF-10 and MCF-7 cell lines treated with 5 mg/ml of nanocomposite. The stars on each column showed a significant difference compared with the control (MCF-10 cell line) and the stars on the lines indicate a significant difference between the various treated cell types. *P*-value<0.05:\*, *P*-value<0.01:\*\*, *P*-value<0.001:\*\*\*, *P*-value<0.0001:\*\*\*\*, n.s.: not significant

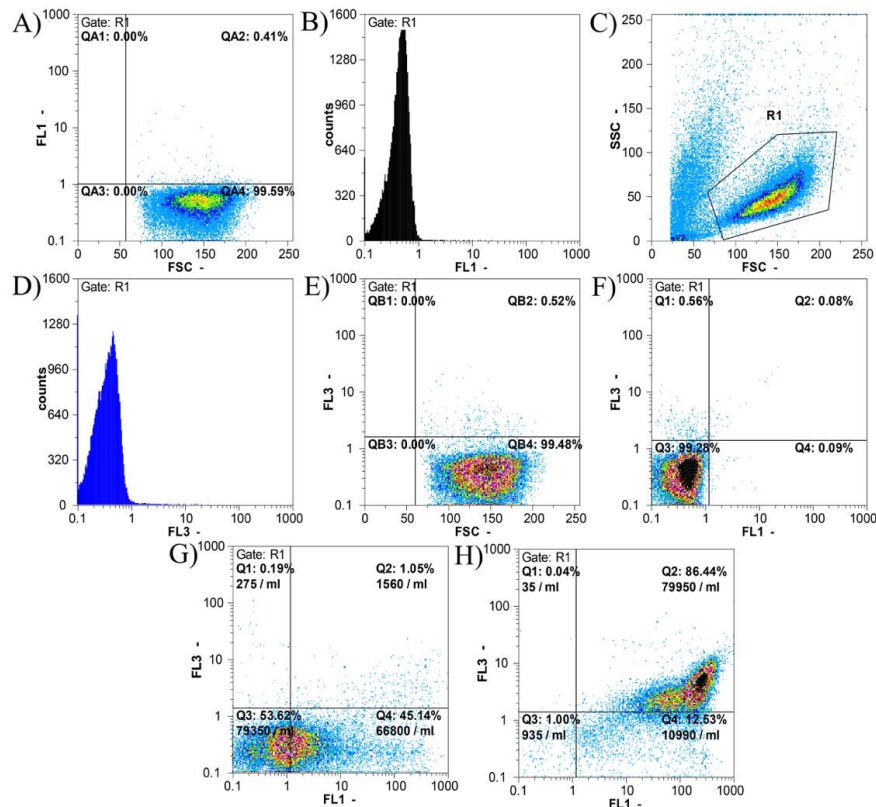


**Figure 5.** Flow cytometric results of apoptosis in MCF-10 and MCF-7 cell lines treated with 0.5 mg/ml of nanocomposite for 48 hr using the Annexin-V-FITC/PI assay. A-F) Flowcytometric results on the normal MCF-10 cell line without nanocomposite treatment. In Figures A and B, the percentage and number of events counted in the FL1 channel, which are related to the Annexin-V-FITC color, are displayed. The method of selecting the population (gating strategy) is shown in Figure C. Figures E and D show the number of events counted in the FL3 channel, which are related to the PI color. In Figure F, based on both Annexin-V-FITC (FL1) and PI (FL3) colors, a quadrant chart is drawn that shows each of the cell groups. In Figures F to I: Q1 is the percentage of necrotic cells, Q2 is the percentage of cells in the late phase of apoptosis, Q3 is the percentage of cells in the early phase of apoptosis and Q4 represents the percentage of live cells. According to the gating strategy shown in section C, the results of apoptosis in other cell lines were calculated. Figures G, and H respectively show the results of apoptosis examination in MCF-10 and MCF-7 cell lines treated with 0.5 mg/ml nanocomposite for 48 hr

and only 0.19% of the cells were necrotic. The apoptotic cell population comprised 46.19% of the cells from which 45.14% were in the early and 1.05% of the cells were in the late apoptosis stage.

The maximum apoptosis induction after treatment with 0.5 mg/ml of nanocomposite for 48 hr was seen in the MCF-7 cell line in which only 1% of the cells were alive and 0.04% of the cells were necrotic. The rest of the cells (98.97%) underwent apoptosis divided into early (12.53%) and late (86.44%) phases.

Comparison of apoptotic, necrotic, and viable cell lines that were exposed for 48 hr to 0.5 mg/ml nanocomposite is shown in Figure 6. As shown, the percentage of live cells is significantly different across both treated cell lines and also with untreated MCF-10. The untreated MCF-10 cell line has the highest number of living cells and among the treated cell lines, MCF-7 had significantly lower living cells. Also, the percentage of apoptotic cells was significantly different between both treated cell lines, as well as the untreated MCF-10 cell line. The untreated MCF-10 cell line had the lowest number of apoptotic cells and also among the treated cell lines, MCF-7 had significantly higher apoptosis. There was no significant difference in the results of necrotic cells between the three groups.

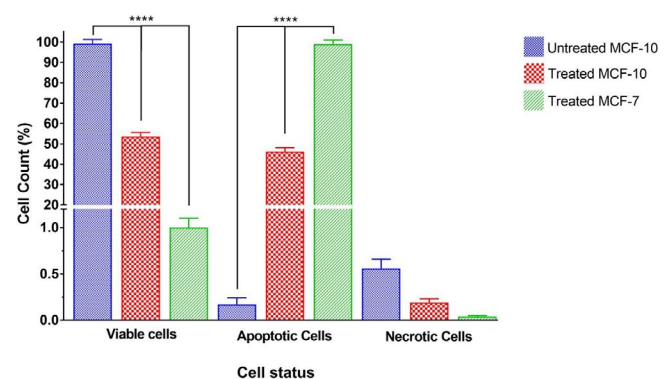


**Figure 6.** Comparison of percentages of live, apoptotic, and necrotic cell lines after treatment with 0.5 mg/ml concentration of nanocomposite for 48 hr. The stars on the lines show the significant difference between the various treated cell lines. P-value<0.0001:\*\*\*\*

## Discussion

This study showed that the 8-HQ-coated GO had high toxicity for MCF-7 breast cancer cell line, while it was very low toxic for MCF-10 normal breast cells. It might indicate the relative specific toxicity of nanocomposite

for cancer cell lines. It was also observed that the effects of the nanocomposite toxicity are dose- and time-dependent.

It has been reported that binding GO to other nanoparticles or chemicals increases its efficacy. For instance, binding SN38 and doxorubicin (DOX) to GO increases solubility, biocompatibility, distribution in tumor tissue and anti-cancer effects (21, 22). One of the biggest problems of GO application is aggregation in physiological solutions which could be solved by binding to other nanomaterials (23). In this study, 8-HQ was coated with a mesoporous silica SBA-15 and then coated with GO.

The toxicity of carbon nanoparticles such as graphene, GO, and carbon nanotubes to different classes of cancerous and normal cells, has been shown and pointed to the role of shape and structure of nanoparticles in their toxicity (15, 24, 25).

Studies have also shown the synergistic effects of GO with other anticancer drugs (26, 27), which was the reason for binding 8-HQ to GO in our study. One of the considerable drawbacks of our study is the lack of individual investigation of silica, GO, and 8-HQ anti-cancer effects separately and comparing with the 8-HQ-coated GO. In this case, we could clearly show the effects of each alone and the synergistic effects of the combination. However, according to the past studies, GO and SBA-15 mesoporous silica have low cytotoxicity effects on MCF-7 or other cell lines introducing them as biocompatible drug delivery systems for anti-cancer treatment (28-30). On the other hand, 8-HQ has been shown to have cytotoxic effects on MCF-7 cell line by itself and in combination with other anti-cancer agents (31).

So far, various nanomaterials have been used as carriers of anticancer drugs (32, 33), of which GO showed more advantages in loading drugs including doxorubicin (34), paclitaxel (27), methotrexate (35), and other drugs in various cancers. Also, the specificity and increased cytotoxicity of GO-bounded doxorubicin in comparison with doxorubicin are shown by MTT and similar assays on cancer cells, including MCF-7 (26, 36). In many of these studies, the effects of GO on normal cells have been reported very rarely, indicating the relative specificity and greater effect of this substance on cancer cells, although the exact mechanism of this difference in effect is still unknown (15). Fiorillo *et al.* (37) showed that GO specifically inhibits the proliferation of cancer cell stem cells (CSCs) in various cancers and is not toxic to the normal pluripotent stem cells, but induces their differentiation into different cell types (37, 38). Given that the cells used in this study were cancer cell stem cells (CSC), one of the causes of the high toxicity of nanocomposites could be the induction of cell differentiation and cell death in these cell lines. Some derivatives of quinolines including 8HQ have anti-cancer properties due to their ability to chelate the bivalent ions needed to grow cancer (39, 40). In our study, the sensitivity of the breast cancer cell line to the 8HQ nanocomposite has been well illustrated. Studies on the MCF-7 cell line provided evidence on the specific effect of quinoline derivatives and showed that breast cancer cells are susceptible to these compounds in the MTT assay (41, 42).

In the present study, the expression of pro-apoptotic

genes in the MCF-7 treated cell line with nanocomposite was higher, compared with control (MCF-10), indicating the effects of nanocomposite on the induction of apoptosis in this cancer cell line. *P21* is one of the crucial genes in inducing cell cycle arrest (6) and increasing its expression in the cancer cell line can increase the probability of nanocomposite-induced cell cycle arrest which requires more confirmatory tests. On the other hand, expression of the anti-apoptotic *BCL2* gene in the treated breast cancer cell line has significantly decreased compared with control cells representing a probable reduction in survival signals in these cancer cells. The Annexin-V/PI assay also indicated that severe apoptosis was induced in breast cancer cells following treatment with nanocomposites, which was significantly higher than that of MCF-10. It might show that the MCF-7 cells are more susceptible to apoptosis induction via 8HQ-GO nanocomposites compared with MCF-10.

The previous studies have shown that cell cycle arrest and apoptosis are mechanisms of cytotoxicity of quinoline derivatives and GO (15, 43). Quinoline derivatives inhibit the signaling pathway of PI3K-Akt-mTOR leading to cell cycle arrest and apoptosis induction in MCF-7 (42). In this study, we observed that the 8HQ-containing nanocomposite has much lower toxicity on normal breast epithelial cells than on cancer cells. In similar studies, 8HQ-titanium complexes in the MTT assay exhibited high cytotoxicity characteristics against BEL-7404, HepG2, NCI-H460, T-24, and A549 cancer cells while little toxicity was found on HL-7702 normal liver cell line. It has also been pointed out that these complexes inhibit cell cycle progression and induce mitochondrial apoptosis (44).

## Conclusion

Conclusively, the 8HQ-coated GO has relatively specific toxicity for MCF-7 breast cancer cell line, while it has much lower toxicity to normal breast epithelial cells. One of the main mechanisms of this cytotoxicity is the induction of apoptosis such that the nanocomposite induced molecular and cellular apoptosis in cancer cells whereas low apoptosis was observed in treated normal breast epithelial cells. The point that should not be overlooked is that all these results were obtained by *in vitro* study on cell lines. The *in vivo* antitumor effects of this nanocomposite should also be investigated. Interestingly, the *in vivo* anti-tumor properties of 8HQ-2-quinoline carbaldehyde were studied on nude male rats bearing hepatocellular carcinoma xenograft tumor (Hep3B) and showed that intraperitoneal injections of nanocomposite have completely stopped the growth of the tumor and caused no tissue damage on the vital organs of the mouse (45). It is suggested to investigate molecular and cellular mechanisms more precisely, including cell proliferation, cell cycle, migration, invasion, metastasis, and angiogenesis following nanocomposite treatment on these cell lines and other cancerous or normal cells to evaluate the specificity of the nanocomposite functions.

## Acknowledgment

The results presented in this paper were part of a student thesis. The study was funded by the Science and Research Branch of Islamic Azad University and

Motamed Breast Cancer Research Center, Tehran, Iran. The authors would like to thank Dr. Hassan Goldooz for his contribution to nanocomposite preparation, Dr. Sepideh Kazemi for her help in experimental tests and Dr. Mohammad Hossein Kazemi for scientific and English editing of the manuscript. All authors read and approved the final manuscript and have no conflicts of interest.

### Conflicts of Interest

The authors declare that there are no conflicts of interest.

### References

- Bray F, Ferlay J, Soerjomataram I, Siegel RL, Torre LA, Jemal A. Global cancer statistics 2018: GLOBOCAN estimates of incidence and mortality worldwide for 36 cancers in 185 countries. *CA cancer J Clin* 2018; 68:394-424.
- Sharma GN, Dave R, Sanadya J, Sharma P, Sharma K. Various types and management of breast cancer: an overview. *J Adv Pharm Technol Res* 2010; 1:109-126.
- Stewart BW. Mechanisms of apoptosis: integration of genetic, biochemical, and cellular indicators. *J Natl Cancer Inst* 1994; 86:1286-1296.
- Dakubo GD. Mitochondrial genetics and cancer: Springer Science & Business Media; 2010.
- El-Deiry WS, Tokino T, Velculescu VE, Levy DB, Parsons R, Trent JM, et al. WAF1, a potential mediator of p53 tumor suppression. *Cell* 1993; 75:817-825.
- Bunz F, Dutriaux A, Lengauer C, Waldman T, Zhou S, Brown J, et al. Requirement for p53 and p21 to sustain G2 arrest after DNA damage. *Science* 1998; 282:1497-1501.
- Fulda S, Debatin K-M. Extrinsic versus intrinsic apoptosis pathways in anticancer chemotherapy. *Oncogene* 2006; 25:4798.
- Pierson HO. Handbook of carbon, graphite, diamonds and fullerenes: processing, properties and applications: William Andrew; 2012.
- Du W, Jiang X, Zhu L. From graphite to graphene: direct liquid-phase exfoliation of graphite to produce single- and few-layered pristine graphene. *J Mater Chem A Mater* 2013; 1:10592-10606.
- Paulchamy B, Arthi G, Lignesh B. A simple approach to stepwise synthesis of graphene oxide nanomaterial. *J Nanomed Nanotechnol* 2015; 6:253-256.
- Wei J, Vo T, Inam F. Epoxy/graphene nanocomposites—processing and properties: A review. *RSC Adv* 2015; 5:73510-73524.
- Srivastava V, Negi AS, Kumar J, Gupta M, Khanuja SP. Plant-based anticancer molecules: a chemical and biological profile of some important leads. *Bioorg Med Chem* 2005; 13:5892-5908.
- Afzal O, Kumar S, Haider MR, Ali MR, Kumar R, Jaggi M, et al. A review on anticancer potential of bioactive heterocycle quinoline. *Eur J Med Chem* 2015; 97:871-910.
- Xu H, Chen W, Zhan P, Liu X. 8-Hydroxyquinoline: a privileged structure with a broad-ranging pharmacological potential. *Med Chem Comm* 2015; 6:61-74.
- Bianco A. Graphene: safe or toxic? The two faces of the medal. *Angew Chem Int Ed Engl* 2013; 52:4986-4997.
- Hummers Jr WS, Offeman RE. Preparation of graphitic oxide. *J Am Chem Soc* 1958; 80:1339-1339.
- Badiei A, Goldooz H, Ziarani GM. A novel method for preparation of 8-hydroxyquinoline functionalized mesoporous silica: Aluminum complexes and photoluminescence studies. *Appl Surf Sci* 2011; 257:4912-4918.
- Goldooz H, Badiei A, Shiravand G, Ghasemi JB, Ziarani GM. A highly selective Ag<sup>+</sup> sensor based on 8-hydroxyquinoline functionalized graphene oxide-silica nanosheet and its logic gate behaviour. *J Mater Sci* 2019; 30:17693-17705.
- Priyadarsini RV, Murugan RS, Maitreyi S, Ramalingam K, Karunakaran D, Nagini S. The flavonoid quercetin induces cell cycle arrest and mitochondria-mediated apoptosis in human cervical cancer (HeLa) cells through p53 induction and NF- $\kappa$ B inhibition. *Eur J Pharmacol* 2010; 649:84-91.
- Livak KJ, Schmittgen TD. Analysis of relative gene expression data using real-time quantitative PCR and the 2- $\Delta\Delta$ CT method. *Methods* 2001; 25:402-408.
- Lei H, Xie M, Zhao Y, Zhang F, Xu Y, Xie J. Chitosan/sodium alginate modified graphene oxide-based nanocomposite as a carrier for drug delivery. *Ceram Int* 2016; 42:17798-17805.
- Liu Z, Robinson JT, Sun X, Dai H. PEGylated nanographene oxide for delivery of water-insoluble cancer drugs. *J Am Chem Soc* 2008; 130:10876-10877.
- Yadav N, Kumar N, Prasad P, Shirbhate S, Sehwat S, Lochab B. Stable dispersions of covalently tethered polymer improved graphene oxide nanoconjugates as an effective vector for siRNA delivery. *ACS Appl Mater Interfaces* 2018; 10:14577-14593.
- Chang Y, Yang S-T, Liu J-H, Dong E, Wang Y, Cao A, et al. *In vitro* toxicity evaluation of graphene oxide on A549 cells. *Toxicol Lett* 2011; 200:201-210.
- Chen L, Hu P, Zhang L, Huang S, Luo L, Huang C. Toxicity of graphene oxide and multi-walled carbon nanotubes against human cells and zebrafish. *Sci China Chem* 2012; 55:2209-2216.
- Alibolandi M, Mohammadi M, Taghdisi SM, Ramezani M, Abnous K. Fabrication of aptamer decorated dextran coated nano-graphene oxide for targeted drug delivery. *Carbohydr Polym* 2017; 155:218-229.
- Liu Y, Zhong H, Qin Y, Zhang Y, Liu X, Zhang T. Non-covalent hydrophilization of reduced graphene oxide used as a paclitaxel vehicle. *RSC Adv* 2016; 6:30184-30193.
- Chaudhari NS, Pandey AP, Patil PO, Tekade AR, Bari SB, Deshmukh PK. Graphene oxide based magnetic nanocomposites for efficient treatment of breast cancer. *Mater Sci Eng C* 2014; 37:278-285.
- Hu W, Peng C, Luo W, Lv M, Li X, Li D, et al. Graphene-based antibacterial paper. *ACS Nano* 2010; 4:4317-4323.
- Krajnović T, Maksimović-Ivanić D, Mijatović S, Drača D, Wolf K, Edeler D, et al. Drug delivery system for emodin based on mesoporous silica SBA-15. *Nanomaterials* 2018; 8:322-337.
- Wang D, Huang J, Wang X, Yu Y, Zhang H, Chen Y, et al. The eradication of breast cancer cells and stem cells by 8-hydroxyquinoline-loaded hyaluronan modified mesoporous silica nanoparticle-supported lipid bilayers containing docetaxel. *Biomaterials* 2013; 34:7662-7673.
- Dreaden EC, Alkilany AM, Huang X, Murphy CJ, El-Sayed MA. The golden age: gold nanoparticles for biomedicine. *Chem Soc Rev* 2012; 41:2740-2779.
- Liu W, Li X, Wong Y-S, Zheng W, Zhang Y, Cao W, et al. Selenium nanoparticles as a carrier of 5-fluorouracil to achieve anticancer synergism. *ACS Nano* 2012; 6:6578-6591.
- Lv Y, Tao L, Bligh SA, Yang H, Pan Q, Zhu L. Targeted delivery and controlled release of doxorubicin into cancer cells using a multifunctional graphene oxide. *Mater Sci Eng C* 2016; 59:652-660.
- Jafarizad A, Aghanejad A, Sevim M, Metin Ö, Barar J, Omid Y, et al. Gold nanoparticles and reduced graphene oxide-gold nanoparticle composite materials as covalent drug delivery systems for breast cancer treatment. *ChemistrySelect* 2017; 2:6663-6672.
- Fan L, Ge H, Zou S, Xiao Y, Wen H, Li Y, et al. Sodium alginate conjugated graphene oxide as a new carrier for drug delivery system. *Int J Biol Macromol* 2016; 93:582-590.
- Fiorillo M, Verre AF, Iliut M, Peiris-Pagés M, Ozsvári B, Gandara R, et al. Graphene oxide selectively targets cancer stem cells, across multiple tumor types: Implications for

- non-toxic cancer treatment, via "differentiation-based nano-therapy". *Oncotarget* 2015; 6:3553-3562.
38. Yoon HH, Bhang SH, Kim T, Yu T, Hyeon T, Kim BS. Dual roles of graphene oxide in chondrogenic differentiation of adult stem cells: Cell-adhesion substrate and growth factor-delivery carrier. *Adv Func Mater* 2014; 24:6455-6464.
39. Prachayasittikul V, Prachayasittikul S, Ruchirawat S, Prachayasittikul V. 8-Hydroxyquinolines: a review of their metal chelating properties and medicinal applications. *Drug Des Devel Ther* 2013; 7:1157.
40. Zhai S, Yang L, Cui QC, Sun Y, Dou QP, Yan B. Tumor cellular proteasome inhibition and growth suppression by 8-hydroxyquinoline and clioquinol requires their capabilities to bind copper and transport copper into cells. *J Biol Inorg Chem* 2010; 15:259-269.
41. Wang N, Świtalska M, Wu MY, Imai K, Ngoc TA, Pang CQ, et al. Synthesis and *in vitro* cytotoxic effect of 6-amino-substituted 11H-and 11Me-indolo [3, 2-c] quinolines. *Eur J Med Chem* 2014; 78:314-323.
42. Xiao Z, Lei F, Chen X, Wang X, Cao L, Ye K, et al. Design, synthesis, and antitumor evaluation of quinoline-imidazole derivatives. *Arch Pharm* 2018; 351:1700407.
43. Chen C, Hou X, Wang G, Pan W, Yang X, Zhang Y, et al. Design, synthesis and biological evaluation of quinoline derivatives as HDAC class I inhibitors. *Eur J Med Chem* 2017; 133:11-23.
44. Qin Q-P, Chen Z-F, Qin J-L, He X-J, Li Y-L, Liu Y-C, et al. Studies on antitumor mechanism of two planar platinum (II) complexes with 8-hydroxyquinoline: synthesis, characterization, cytotoxicity, cell cycle and apoptosis. *Eur J Med Chem* 2015; 92:302-313.
45. Chan SH, Chui CH, Chan SW, Kok SHL, Chan D, Tsoi MYT, et al. Synthesis of 8-hydroxyquinoline derivatives as novel antitumor agents. *ACS Med Chemlett* 2012; 4:170-174.